Journal of Molecular Catalysis A: Chemical 339 (2011) 72–78

Contents lists available at ScienceDirect

Journal of Molecular Catalysis A: Chemical

journal homepage: www.elsevier.com/locate/molcata

New chiral Schiff base–zinc complexes and their esterolytic catalytic activity

Ramu Kannappan, Masaomi Matsumoto, John Hallren, Kenneth M. Nicholas*

Department of Chemistry and Biochemistry, Stephenson Life Sciences Research Center, 101 Stephenson Parkway, University of Oklahoma, Norman, OK 73019, USA

ARTICLE INFO

Article history:
Received 14 January 2011
Received in revised form 14 February 2011
Accepted 18 February 2011
Available online 26 February 2011

Keywords:
Chiral Schiff base
Zinc catalyst
Ester alcoholysis

ABSTRACT

A new series of chiral Zn–Schiff base (imine) complexes has been prepared from mono-*N*-sulfonyl derivatives of (1R,2R)-diaminocyclohexane, *N*-heterocyclic aldehydes, and zinc salts. The formation and characterization of the (L)ZnX_2 complexes was established by NMR, IR and HRESI-MS. Spectroscopic and kinetic evidence indicates that these ligands may be bidentate or tridentate depending on conditions of the medium. The methanolysis of a chiral, racemic picolinate ester catalyzed by the Zn(II)–Schiff base complexes was studied kinetically. The rate constants were found to vary approximately a hundred-fold and in a complex way depending on the imine ligand and the Zn-counter anion, $k_{obs} = 5.0 \times 10^{-6}$–$4.8 \times 10^{-4}$ M^{-1} s^{-1}. A Job plot analysis of ternary complex formation of LZnX_2 with two phosphonate transition state analogs suggests that two types of (imine)Zn(picolinate)*X* ternary complexes may be intermediates and that varying rate-limiting steps may be involved in the LZnX_2-catalyzed methanolysis of picolinate esters.

1. Introduction

In biological systems metalloprotease and -esterase enzymes catalyze the hydrolysis of amides and esters with remarkable efficiency by making use of the protein-ligated metal center to electrophilically activate the substrate and, in some cases, to increase the acidity and the nucleophilicity of coordinated water [1]. For example, carboxypeptidase A and thermolysin are Zn(II)-metalloenzymes that catalyze the hydrolysis of peptides and O-acyl derivatives of α-hydroxycarboxylic acids [2,3]. The zinc cation in the active site adopts a tetrahedral coordination geometry attached to the protein backbone by three amino acid residues, two histidine imidazoles and an aspartate or glutamate carboxylate, with the fourth coordination site occupied by a water molecule. The ubiquity of zinc in metalloenzymes chemistry has been related to its flexible coordination chemistry, substitutional lability, Lewis acidity, intermediate polarizability and lack of redox activity [4]. To better understand the factors that control the detailed properties of the active sites of zinc enzymes, numerous model complexes have been investigated [5]. Studies of scorpionate– and other tripodal–Zn complexes have led to the elucidation of key mechanistic features of the catalysis by Zn-enzymes [6]. These include biomimetic hydrolyses as well as the modeling of intermediates of peptidase and carbonic anhydrase catalytic cycles [7].

The hydrolysis and alcoholysis of esters, often possessing coordinating co-functionality, can be catalyzed by divalent metal ions such as Co^{2+}, Ni^{2+}, Zn^{2+} and Cu^{2+} with k_{cat}/k_{uncat} values as large as 10^8 [8]. The facility of hydrolytic reactions of picolinate esters has found use in organic synthesis, as a protecting group for alcohols (deprotected by MeOH/$Zn(OAc)_2$) [9] and in the Mitsunobu stereoinversion of alcohols (the picolinate removed by MeOH/$Cu(OAc)_2$) [10]. Particularly valuable hydrolytic reactions are those that are stereoselective, including kinetic resolutions. Biocatalytic enantioselective hydrolysis, alcoholysis and transesterification reactions have achieved good efficiencies and are applied in the industrial production of optically active compounds, yet, their substrate scope is often limited [11]. In contrast, the development of enantioselective hydrolysis, alcoholysis or transesterification reactions using homogeneous metal complex catalysts has been quite limited with the most notable success being achieved for the kinetic resolution of alkenyl esters, ethers and azlactones [12] and of epoxides [13].

We recently reported a new method for the evolution of hydrolytic catalysts by templating a set of imine–metal complexes, in equilibrium with their constituent aldehydes and amines, with transition state analogs [14]. A good correlation between (imine)Zn(TSA) ternary complex formation and the hydrolytic activity of the (imine)ZnX_2 complexes was found as predicted by the Pauling–Jenks model for enzyme and antibody catalysis [15]. On the way to developing applications of this new homogeneous catalyst selection technology we hypothesized its potential use for the kinetic resolution of chiral, racemic alcohols via their picolinate esters, employing homochiral imine–metal complex catalysts and suitable TSAs. Herein, we report the preparation of new Zn-complexes of chiral, Schiff base (imine) ligands and their efficacy as catalysts for the methanolysis of a chiral picolinate ester.

* Corresponding author. Tel.: +1 405 325 3696; fax: +1 405 325 6111.
E-mail address: knicholas@ou.edu (K.M. Nicholas).

1381-1169/$ – see front matter © 2011 Elsevier B.V. All rights reserved.
doi:10.1016/j.molcata.2011.02.014

2. Experimental

2.1. Materials and general methods

Commercially available reagents were used as received. (Rac)-1-phenylethanol picolinic acid ester (PEP), (S)-1-phenylethanol pyridinephosphonic acid ester [16] (PEPP = TSA), and 8-isopropyl-2-quinolinecarboxaldehyde [17] were prepared according to the literature procedures. (1*R*,2*R*)-*N*-(*N*,*N*-dimethylsulfamoyl)-1,2-diaminocyclohexane (**1c**) was prepared and purified as previously [18]. Infrared spectra (4000–500 cm^{-1}) were recorded using KBr pellets. ^1H (300 MHz) and ^{13}C (60 MHz) NMR spectra were obtained and referenced to TMS as an internal standard. The low- and high-resolution mass spectra were acquired on samples dissolved in methanol or dichloromethane solution by the ESI ionization method.

2.2. Synthetic procedures

2.2.1. Preparation of *N*-(2-amino-cyclohexyl)-4-methyl-benzenesulfonamide (*1a*) and *N*-(2-amino-cyclohexyl)-2,4,6-trimethyl-benzenesulfonamide (*1b*)

The sulfonamides **1a** and **1b** were prepared from *trans*-(R,R)-1,2-diaminocyclohexane directly rather than as its L-tartrate salt as previously reported [19]. To a stirred solution of (R,R)-1,2-diaminocyclohexane (3.00 g, 11.4 mmol) in aqueous NaOH (2 N, 15 mL) was added triethylamine (2.1 mL, 15.2 mmol) and dichloromethane (100 mL). The mixture was cooled to 0 °C and a solution of p-toluene- or 2,4,6-trimethylphenyl (mesityl) sulfonyl chloride (7.6 mmol) in dichloromethane (50 mL) was added dropwise over 30 min. After the addition was complete, the mixture was allowed to warm to rt and stirred for 12 h. The resulting mixture was washed with aqueous HCl (2 N, 3 × 50 mL) and the organic phase was removed. The aqueous phase was adjusted to pH 9 by addition of NaOH pellets and the basic aqueous solution was then extracted with dichloromethane (3 × 30 mL). The dichloromethane layers were combined, dried over anhydrous $MgSO_4$, filtered, and the solvent was removed under reduced pressure to obtain **1a** and **1b** as yellow solids. The NMR spectra for **1a**–**c** agreed with the earlier reports [18,19].

2.2.2. Preparation of Zn complexes

The synthesis of **2a** is described below and the compounds **2b**–**2i** were prepared using the same procedure. Monosulfonamide derivative **1a** was dissolved in methanol (0.50 mmol, 50 mL). To this solution a methanolic solution of 2-pyridinecarboxaldehyde (0.50 mmol, 25 mL) was added, followed by the appropriate zinc salt dissolved in methanol (0.50 mmol, 25 mL). The resulting mixture was refluxed overnight, then the solvent was evaporated and the residual solid was triturated with small portions of diethyl ether to obtain the spectroscopically pure product **2a**.

(2a) ESI-HRMS (CH_3OH) found: m/z = 456.0504, calcd for $C_{19}H_{23}N_3O_2SZnCl^+$ = 456.0491; IR (KBr): 3241, 2863, 1643, 1331, 1159; ^1H-NMR (CD_3CN, δ_{ppm}): 8.69 (d, J = 4.8 Hz, 1H), 8.34 (s, 1H), 8.21 (m, 1H), 7.83 (m, 1H), 7.75 (d, J = 7.5 Hz, 1H), 7.63 (d, J = 8.4 Hz, 1H), 7.0 (d, J = 8.1 Hz, 2H), 5.35 (s, 1H), 3.20 (m, 1H), 3.30 (m, 1H) 2.19 (s, 3H), 1.73–1.97 (m, 4H), 1.32–1.17 (m, 4H).

(**2b**) ESI-HRMS (CH_3OH) found: m/z = 459.0526, calcd for $C_{18}H_{24}N_4O_2S^{64}ZnCl^+$ = 459.0600; IR (KBr): 3245, 2863, 1626, 1327, 1151; ^1H-NMR (CD_3CN, δ_{ppm}): 8.26 (s, 1H), 7.72 (d, J = 8.1 Hz, 2H), 7.31 (d, J = 1.2 Hz, 1H), 7.21 (br, 1H), 7.07 (d, J = 8.1 Hz, 2H), 5.45 (s, 1H), 3.66 (s, 3H), 3.42 (m, 2H), 2.29 (s, 3H), 1.98–1.96 (m, 4H), 1.32–1.17 (m, 4H).

(**2c**) ESI-HRMS (CH_3OH) found: m/z = 611.1237, calcd for $C_{30}H_{32}N_4O_2S^{64}ZnCl^+$ = 611.1226; IR (KBr): 3245, 2863, 1618, 1327, 1155, ^1H-NMR (CD_3CN, δ_{ppm}): 8.43 (s, 1H), 7.78 (d, J = 8.1 Hz, 2H), 7.73 (d, J = 7.5 Hz, 2H), 7.60–7.54 (m, 4H), 7.51–7.34 (m, 4H), 7.20 (d, J = 7.5 Hz, 2H), 3.60 (s, 3H), 3.45 (m, 1H), 2.93 (m, 1H), 2.44 (s, 3H), 1.98–1.96 (m, 4H), 1.41–1.13 (m, 4H).

(**2d**) ESI-HRMS (CH_3OH) found: m/z = 548.1153, calcd for $C_{26}H_{31}N_3O_2S^{64}ZnCl^+$ = 548.1117; IR (KBr): 3257, 2859, 1612, 1331, 1155; ^1H-NMR (CD_3OD, δ_{ppm}): 8.34 (s, 1H), 8.15 (d, J = 8.4 Hz, 1H), 7.76–7.74 (m, 1H), 7.70–7.65 (m, 2H), 7.57 (d, J = 7.5 Hz, 1H), 7.47 (d, J = 8.1 Hz, 2H), 6.76 (d, J = 7.5 Hz, 2H), 4.35 (septet, J = 6.6 Hz, 1H), 3.40 (m, 1H), 3.20 (m, 1H), 1.88 (s, 3H), 1.74 (d, J = 6.0 Hz, 6H), 2.07–1.33 (m, 8H).

(**2e**) ESI-HRMS (CH_3OH) found: m/z = 626.1293, calcd for $C_{28}H_{31}N_3O_4S^{64}ZnF_3^+$ = 626.1279; IR (KBr): 3277, 2863, 1701, 1450, 1331, 1194; ^1H-NMR (CD_3CN, δ_{ppm}): 8.43 (d, J = 8.1 Hz, 1H), 8.01 (s, 1H), 7.87–7.69 (m, 3H), 7.55 (d, J = 8.4 Hz, 1H), 7.40 (d, J = 8.1 Hz, 2H), 6.93 (d, J = 6.9 Hz, 2H), 5.56 (b, 1H), 4.50 (septet, J = 6.6 Hz, 1H), 3.45 (m, 1H), 3.0 (m, 1H), 2.26 (s, 3H), 1.97 (d, J = 5.4 Hz, 6H), 2.01–1.74 (m, 4H), 1.74–1.44 (m, 4H).

(**2f**) ESI-HRMS (CH_3OH) found: m/z = 662.0933, calcd for $C_{27}H_{31}N_3O_5S_2{}^{64}ZnF_3^+$ = 662.0949; IR (KBr): 3227, 2870, 1612, 1330, 1159; ^1H-NMR (CD_3CN, δ_{ppm}): 8.43 (s, 1H), 7.8 (d, J = 8.1 Hz, 1H), 7.86 (m, 1H), 7.82 (m, 1H), 7.75 (m, 1H), 7.74 (d, J = 7.5 Hz, 1H), 7.75 (d, J = 8.7 Hz, 2H), 7.40 (d, J = 8.4 Hz, 2H), 6.70 (br 1H), 4.45 (septet, J = 6.9 Hz, 1H), 3.07 (m, 2H), 2.42 (s, 3H), 1.70–1.40 (m, 4H), 1.39 (d, J = 6.9 Hz, 6H), 1.30–1.20 (m, 4H).

(**2g**) ESI-HRMS (CH_3OH) found: m/z = 506.0682, calcd for $C_{23}H_{25}N_3O_2S^{64}ZnCl^+$ = 506.0647; IR (KBr): 3245, 2853, 1643, 1323, 1155; ^1H-NMR (CD_3CN, δ_{ppm}): 8.80 (d, J = 8.7 Hz, 1H), 8.52 (s, 1H), 8.28 (d, J = 8.7 Hz, 1H), 8.23 (d, J = 8.1 Hz, 1H), 8.11 (m, 1H), 7.91 (m, 1H), 7.84 (d, J = 8.4 Hz, 1H), 7.59 (d, J = 8.0 Hz, 2H), 6.72 (d, J = 8.4 Hz, 2H), 4.91 (s, 1H), 3.65 (m, 1H), 3.50 (m, 1H), 2.20 (s, 3H), 2.35–1.80 (m, 4H), 1.60–1.28 (m, 4H).

(**2h**) ESI-HRMS (CH_3OH) found: m/z = 654.1624, calcd for $C_{30}H_{35}N_3O_4S^{64}ZnF_3^+$ = 654.1592; IR (KBr): 3223, 2859, 1601, 1319, 1194; ^1H-NMR (CD_3OD, δ_{ppm}): 8.29 (s, 1H), 8.05 (d, J = 8.7 Hz, 1H), 7.70 (d, J = 8.4 Hz, 1H), 7.64 (d, J = 6.6 Hz, 1H), 7.54 (m, 1H), 7.48 (d, J = 8.4 Hz, 1H), 6.30 (s, 2H), 5.17 (s, 1H), 4.36 (septet, J = 6.8 Hz, 1H), 3.32 (m, 1H), 3.12 (m, 1H), 2.60 (s, 3H), 2.42 (s, 6H), 3.20–2.8 (m, 4H), 1.66 (d, J = 6.3 Hz, 6H), 1.80–1.20 (m, 4H).

(**2i**) ESI-HRMS (CH_3OH) found: m/z = 564.1211, calcd for $C_{25}H_{31}N_5O_2S^{64}ZnCl^+$ = 564.1178; IR (KBr): 3227, 2942, 1618, 1331, 1147; ^1H-NMR (CD_3CN, δ_{ppm}): 8.80 (s, 1H), 7.58–7.56 (m, 4H), 7.74–7.25 (m, 6H), 3.76 (s, 3H), 3.45 (m, 1H), 3.25 (m, 1H), 2.80 (s, 3H), 2.67 (s, 3H), 2.30–1.70 (m, 4H), 1.60–1.30 (m, 4H).

2.3. Kinetics for methanolysis of 1-phenylethyl picolinate (PEP) catalyzed by Zn–imine complexes

The methanolysis of *rac*-1-phenylethyl picolinate (PEP) was carried out three times consecutively at the same substrate/catalyst concentration; the listed rate constant (Table 1) is the average from the three runs. A 100 mM stock solution was prepared by dissolving 22.7 mg of *rac*–PEP in 1 mL of CD_3OD/CD_2Cl_2 (1:1). A 20 mM solution of the Zn-complex was prepared in 1.0 mL of 1:1 CD_3OD/CD_2Cl_2. A 1.0 mM stock solution of the complex (Cat-1) was prepared by diluting 50 μL of the 20 mM solution to 1 mL with CD_3OD/CD_2Cl_2 (1:1); A 10 mM stock solution of the complex (Cat-2) was prepared by diluting 500 μL of the 20 mM solution to 1 mL with CD_3OD/CD_2Cl_2 (1:1). Samples for NMR reaction monitoring were prepared by pipetting 100 μL of 100 mM substrate stock solution into an NMR tube and diluting it to 1 mL with CD_3OD/CD_2Cl_2 (1:1); then 100 μL of the catalyst solution (Cat-1 or Cat-2) was added. NMR spectra were recorded at 2-min intervals (T = 292 K) while monitoring the disappearance of the substrate methyl signal at 1.95 ppm and the emergence of the product alcohol methyl

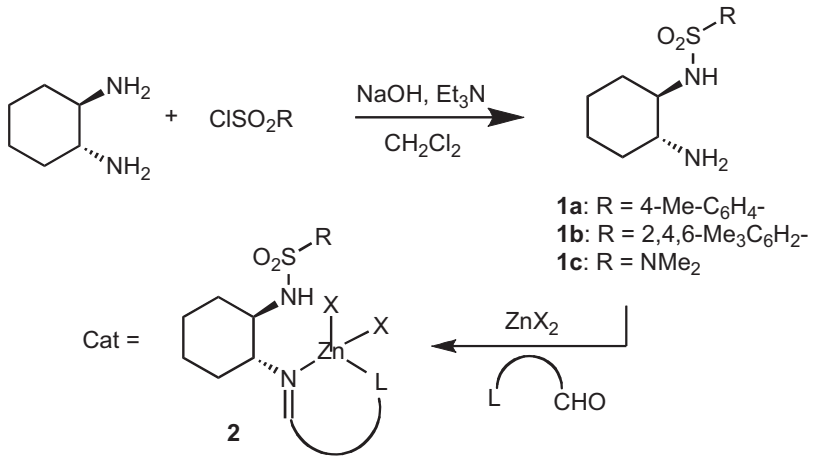

Scheme 1.

peak at 1.69 ppm for up to 20% conversion. Initial rates were determined by plotting the peak integrals versus time (s) for the first 10–15% conversion; the slopes of these plots (averaged for three runs) divided by the initial concentrations of PEP and the Zn-complex **2a–i** provided the second order rate constants listed in Table 1.

Separate kinetic runs of the methanolysis of *R*-PEP and *S*-PEP catalyzed by the same chiral Zn-complex, e.g. **2h**, were conducted as described above. In these experiments the rate constants for the reactions of the *R*- and *S*-PEP were within +10% of each other.

2.4. Deprotonation of $LZnX_2$

The zinc complexes (25 mg **2b**; 29 mg **2d** and 37 mg **2e**) were separately dissolved in 900 μL of CD_3CN, the solutions added to NMR tubes, and their ^{1}H NMR spectra recorded. A 100 μL portion of 0.50 M sodium methoxide (1.0 equiv.) in methanol was then added to each tube via syringe and the ^{1}H-NMR spectrum of each sample was recorded. The peak corresponding to the sulfonamide NH (broad singlet, 5.73 ppm) of **2b** almost completely disappeared after treatment with sodium methoxide. Only partial deprotonation was observed (ca. 50%) for **2d** and **2e**; addition of 2 equiv. of sodium methoxide to 2d caused the sulfonamide NH peak to disappear with some precipitate forming.

*Methanolysis of PEP by deprotonated **2b***: A 10 μL sample of the above solution of deprotonated 2b (10 mol%) was added to a solution of 10 mM *rac*-PEP (or *R*- or *S*-PEP) in CD_3OD/CD_2Cl_2 (1:1 v/v). ^{1}H-NMR spectra of the solution were used as above to monitor the disappearance of substrate and appearance of product. A rate constant of 3.0×10^{-5} M^{-1} s^{-1} was determined, virtually identical to that obtained with the original (non-base treated) complex **2b** as catalyst

Table 1
Rate constants for methanolysis of *rac*-PEP catalyzed by Zn-complexes **2**.

Entry	Catalyst (loading)	k_{rac} (M^{-1} s^{-1})[a]
1	**2a** (10 mol%)	1.4×10^{-5}
2	**2b** (10 mol%)	2.6×10^{-5}
3	**2c** (10 mol%)	5.0×10^{-6}
4	**2d** (1 mol%)	4.8×10^{-4}
5	**2e** (1 mol%)	5.6×10^{-5}
6	**2f** (1 mol%)	6.4×10^{-5}
7	**2g** (1 mol%)	1.7×10^{-4}
8	**2h** (1 mol%)	1.9×10^{-4}
9	**2i** (10 mol%)	–

[a] The rate constants were determined by ^{1}H NMR integration of the growing doublet signal of the product methyl group from three independent runs; [*rac*-PEP]$_0$ = 10 mM, [**2**] = 1.0 mM or 0.1 mM in 1:1 CD_3OD/CD_2Cl_2 (T = 292 K).

2.5. Analysis of $LZnX_2$(TSA) ternary complex formation

Job plot analysis: A 10 mM stock solution of the $LZnX_2$ complex 2 was prepared in 1.5 mL of C_6D_6/CD_3OD (2:1); a 10 mM stock solution of *S*-TSA was prepared in 1.5 mL of C_6D_6/CD_3OD (2:1). The NMR Job plot samples were prepared by combining the zinc complex and *S*-TSA stock solutions in the proportions 450 μL/50 μL, 350 μL/150 μL, 250 μL/250 μL, 150 μL/350 μL, 50 μL/450 μL, keeping the total concentration of $LZnX_2$ plus *S*-TSA constant at 10 mM. Samples were analyzed by ^{1}H-NMR monitoring of the chemical shift (δ) of the p-toluenesulfonamide aromatic proton signals as a function of the Zn/TSA ratio. The plots of $\Delta\delta \times [cat]^0$ versus $[cat]^0/([cat]^0 + [S\text{-PEPP}]^0)$ for **2b** and **2g** are given in Fig. 3.

*ESI–MS of ternary complex from deprotonated **2b***: Complex **2b** (25 mg) in 900 μL methanol (50 mM) was treated with sodium methoxide in methanol (1 equiv.); a 50 mM solution of phenyl 2-pyridylphosphonate (TSA') was prepared in methanol. A 100 μL portion of each solution was added to 800 μL methanol and then analyzed by ESI–MS; found (m/z) = 658.13, 660.15, 662.15; calculated for (**2b**)^{64}Zn(TSA)$^+$, $C_{29}H_{33}N_5O_5PS^{64}Zn$: 658.12

3. Results and discussion

3.1. Preparation and characterization of the complex catalysts

The zinc complexes were prepared by combining a monosulfonamide derived from *trans*-1,2-*R,R*-cyclohexyldiamine (**1a–c**) with one of several *N*-heterocyclic aldehydes, and a zinc salt in methanol (Scheme 1, Fig. 1). The reaction products obtained after workup were analyzed spectroscopically to confirm complex formation and to probe their structures. Their ^{1}H-NMR spectra in CD_3CN or CD_3OD exhibited signals for the N=C–H proton at 8.0–8.8 ppm and for the –$NHSO_2R$ proton at ca. 5.8 ppm, indicating binding of the Schiff base ligands in a bidentate fashion in these solvents. This is noteworthy in light of the role of sulfonamides as inhibitors of Zn-enzymes, which is established to involve Zn-*N,O*-binding to the N-H deprotonated (anionic) form of the sulfonamide [20]. Although the pK_a of Zn-bound sulfonamides isn't established, it is likely to be substantially lower than that of the free sulfonamide (pK_a ca. 10) [21].

The potential for the imine ligands of complexes **2** to achieve tridentate coordination by the deprotonated sulfonamide nitrogen was examined by NMR analysis upon treatment with NaOMe (Scheme 2). The reaction of **2b** with 1 equiv. sodium methoxide resulted in the almost complete disappearance of the sulfonamide NH resonance (broad singlet, 5.73 ppm). However, only partial deprotonation (ca. 50%) was observed for **2d** and **2e** with 1 equiv.

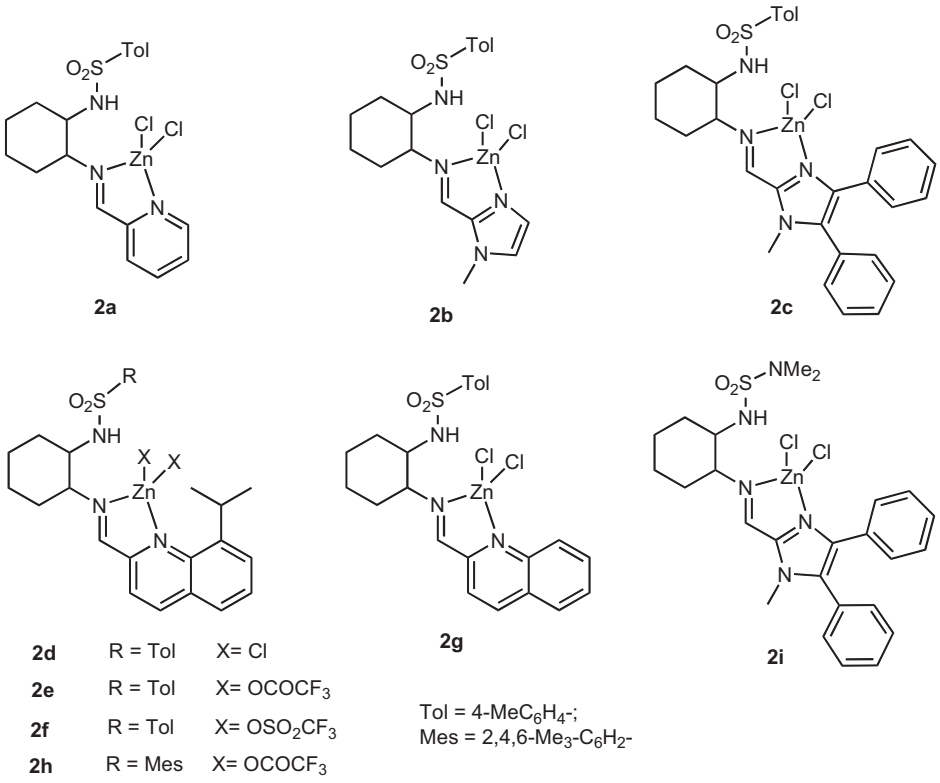

Fig. 1. Chiral Schiff base–ZnX_2 complexes.

of sodium methoxide; with 2 equiv. of NaOMe the sulfonamide NH peak of **2d** disappeared.

The infrared spectra of the Zn(II) complexes **2a**–**2i** provide additional information about the metal-ligand coordination mode. A sharp but weak peak centered in the 3220–3280 cm^{-1} region is most likely due to the N–H stretching vibration of the sulfonamide group. The strong $\nu_{(C=N)}$ bands observed at 1601–1628 cm^{-1} for **2a**–**2i** are shifted considerably towards lower frequencies compared to that of the free Schiff base (1643 cm^{-1}), indicating that the azomethine nitrogen atom is coordinated to the metal [22]. The coordination mode of the trifluoroacetate ions in **2e** and **2h** has been determined from the difference in energy (Δ) between the asymmetric and symmetric carboxylate stretching frequencies. In general, Δ for a monodentate carboxylate is greater than 150 cm^{-1} and for a bidentate carboxylate it is less than 100 cm^{-1}, whereas Δ for a bridging carboxylate is close to 150 cm^{-1} [23]. For the trifluoroacetate complexes (**2e**, **h**) Δ is 251 and 260 cm^{-1} respectively, indicative of monodentate coordination and a Zn-coordination number of four.

Positive mode ESI–MS analysis (CH_3OH solvent) was used to probe further the composition and ionizability of the $LZnX_2$ species. A major peak cluster corresponding to $LZnX^+$ was observed in all the spectra of **2**, indicating that one anionic ligand is labile, creating a cationic species without $(RSO_2)N$–H deprotonation. However, since proton loss would produce a neutral, MS-undetectable (L–H)ZnX species, we cannot determine whether such a process occurs. In some cases low intensity peaks corresponding to $[LZnX(solvent)]^+$ were also detected; e.g. for **2i** at *m*/*z*: 595.12 $[L^{64}ZnCl(MeOH)]^+$.

Attempts to obtain X-ray quality crystals of the LZn(TSA)X complexes for molecular structure determination have been unsuccessful thus far.

3.2. Ester methanolysis

The long term goal of this project is to elicit catalysts for the enantioselective reactions of racemic esters via dynamic templating with transition state analogs. However, the ligand effects on the catalytic activity and mechanisms of metal-ion catalyzed hydrolysis/alcoholysis of picolinates have received little attention [14]. Therefore, before investigating the formation of ternary complexes via TSA-templating, we first examined the catalytic activity of the chiral binary (L)ZnX_2 complexes **2a**–**2i** for the methanolysis of the racemic substrate *rac*-PEP. Reactions of the ester were conducted

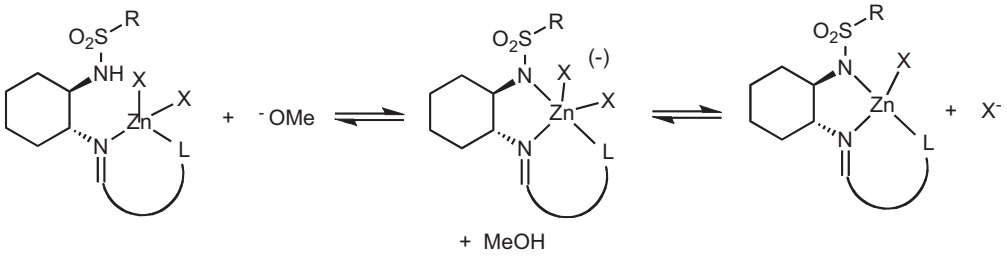

Scheme 2.

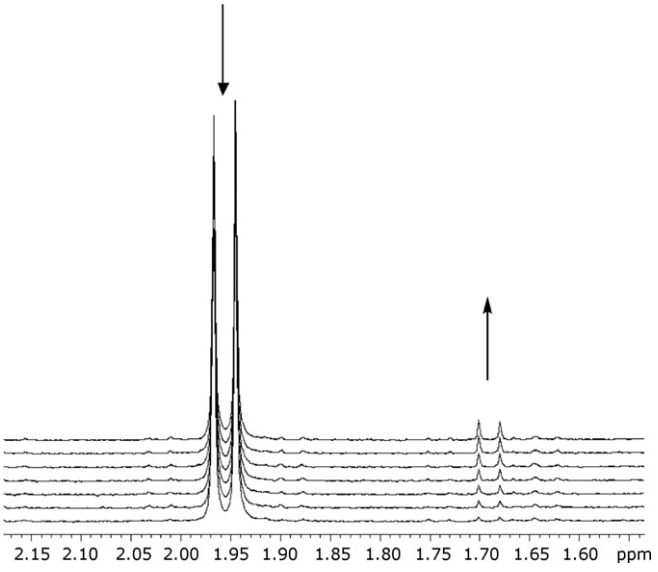

Fig. 2. Time-dependent ^{1}H NMR spectra of *rac*-PEP reaction in CD_3OD/CD_2Cl_2 (1:1) with 1 mol% of **2d** spectra, recorded at 2-min intervals.

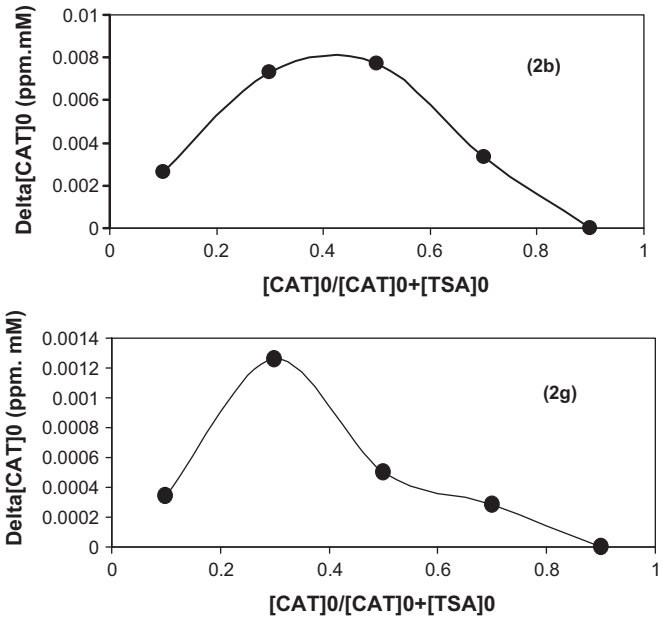

Fig. 3. Job plots for the complexation of **2b** and **2g** with *S*-TSA at a total concentration of 10 mM in C_6D_6/CD_3OD (2:1).

in 10 mM 1:1 CD_3OD/CD_2Cl_2 at 292 K with 1 and 10 mol% catalyst loading. The reaction progress was conveniently monitored by ^{1}H NMR via the decreasing/increasing signals of the methyl groups of the reactant and product respectively (see Fig. 2). Data were collected at low conversion (0–20%) to limit product inhibition and the rate constants were determined by initial rate methods (Table 1).

The rate constants for the methanolysis of *rac*-PEP catalyzed by the $LZnX_2$ complexes **2a**–**i** (Table 1) were found to vary over a substantial range, depending significantly on the imine ligand, the counterion and the sulfonamide group. Considering first the effect of varying the imine ligand (with constant $NHSO_2Tol$ and Cl anionic ligand), i.e. **2a**–**2d** and **2g**, the catalytic activity ranges approximately 100-fold in the order **2b** > **2g** > **2b** > **2a** > **2c** but without an apparent simple correlation with the electronic character or the steric demand of the imine ligand. Whereas complexes of the less basic quinoline ligands, **2d**, **2g** (pK_a 4.6–4.8 [24]), are considerably more active than the pyridine-based complex **2a** (pK_a 5.2 [25]), the complex of the more basic imidazole **2b** (pK_a 7.2) has intermediate activity. Additionally, the most active complex of all, **2d**, is derived from the sterically hindered 8-isopropyl quinoline ligand. Variation of the anionic ligand X (with constant imine and NHTos groups) in the set of quinoline-derived complexes **2d**–**f** shows a nearly 10-fold range of activity in the order **2d** > **2f** > **2e**. This sequence does not correlate with the pK_a of the corresponding acids (pK_a: HCl −7, CF_3CO_2H 0.3, CF_3SO_3H −14 [26]), which would normally relate to the M–X dissociability [27]. The esterolytic catalytic activities of the complexes 2 also depend significantly on the nature of the sulfonamide unit as illustrated by the pairs **2h** > **2e** and **2c** > **2i** (inactive). This suggests a role for coordination of the $–NSO_2R$ unit and is supported by the deprotonation experiments described below. Curiously, with the **2h**/**2e** pair the more hindered mesityl derivative shows greater activity, while the complex **2i**, having the electron rich and presumably less acidic $–NHSO_2NMe_2$ group, is virtually inactive *vis a vis* the –NHTs counterpart **2c**.

3.3. The nature of catalytically relevant LZn-complexes

An issue key to understanding the structure/activity behavior of the $LZnX_2$ complexes is the coordination state of the catalyst species, including whether the imine ligand is bi- or tridentate. Although the complexes **2a**–**h** as prepared in methanol solution apparently have bidentate imine coordination, we found that deprotonation of the sulfonamide nitrogen with probable tridentate coordination is achievable by reaction with methoxide base. To establish whether such deprotonated/tridentate species are viable catalyst intermediates, the esterolytic activity of the deprotonated **2b** was determined, $k_{cat} = 3.0 \times 10^{-5}$ M^{-1} s^{-1}. This value is comparable to that of **2b** in the absence of base ($k_{cat} = 2.5 \times 10^{-5}$ M^{-1} s^{-1}), consistent with the deprotonated $–NSO_2R$ complex being a common catalyst species in both reactions.

To gain further insight into the nature of possible catalytic intermediates the stoichiometries of ternary complexes between the (imine)ZnX_2 complexes and esterolytic transition state analogs were investigated. A Job plot study of the interaction of complexes **2b** or **2e** with the phosphonate transition state analog *S*-TSA by ^{1}H NMR revealed primarily the formation of 1:1 ternary complexes **2b**(*S*-TSA) and **2e**(*S*-TSA) (Fig. 3). In the case of **2g** + *S*-TSA, a major species of 1:2 stoichiometry, 2g$(S\text{-TSA})_2$, apparently is produced. This may be due to the stronger Lewis acidity of **2g** afforded by the less basic quinoline donor versus the imidazole of **2b** and its more accessible Zn-center relative to that having the isopropyl-quinoline ligand of **2e**.

The viability of LZn(picolinate)X species with tridentate imine ligand coordination was tested by examining the interaction of a deprotonated LZnX complex with a transition state analog. Thus $LZnCl_2$ complex **2b** was treated first with NaOMe followed by the addition of the TSA, phenyl pyridylphosphonate. ESI–MS analysis of the resulting solution detected a major species of composition (**2b**)Zn$(TSA)^+$ (Scheme 3b), confirming the formation of a ternary complex between the deprotonated binary complex and the TSA.

3.4. Putative catalytic scheme

Based on the complex structure/catalytic activity results, deprotonation experiments, TSA binding analysis and prior studies of metal catalyzed-picolinate solvolysis, we suggest a tentative mechanistic scheme outlined in Scheme 4. The primary steps involve: (1) coordination of the picolinate substrate (with X^- dissociation); (2) sulfonamide deprotonation/association with X dissociation; either (3) coordination of methanol, followed by (4) inner sphere attack of Zn–OMe on the coordinated ester; or (5) direct (outer sphere) MeOH (or MeO^-) attack on the coordinated carboxyl group; (6)

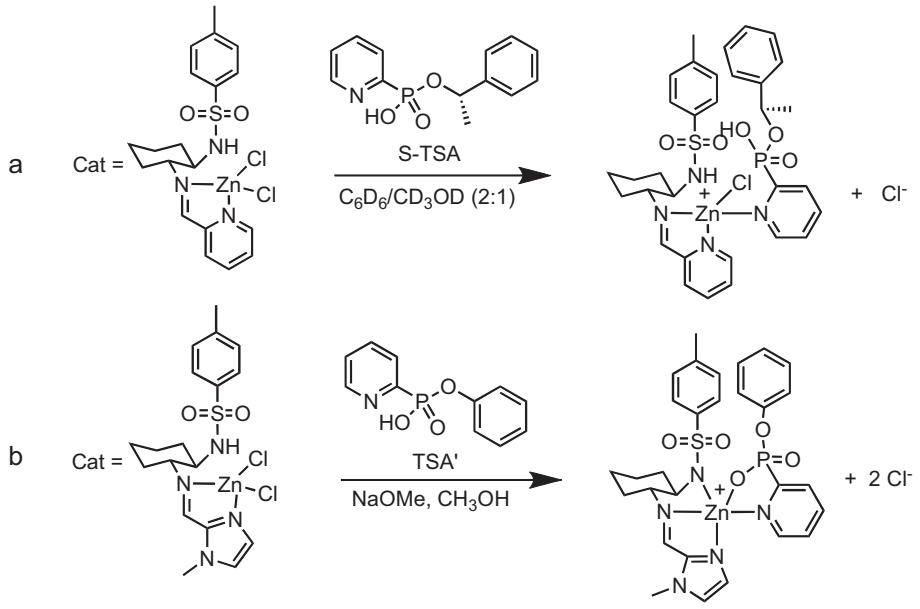

Scheme 3.

collapse of the tetrahedral intermediate to the product alcohol and ester complex; and (7) product ester dissociation followed by substrate ester re-association. We suggest that sulfonamide deprotonation under the catalytic conditions could be driven by the basic pyridine substrate, present in excess relative catalyst. Although we have not established here which step(s) is/are turnover-limiting, previous studies of metal ion-catalyzed ester/amide solvolysis have implicated either outer sphere MeOH(H_2O) addition to Zn-coordinated ester or inner sphere addition of coordinated-hydroxide/alkoxide as rate-limiting [28]. Additional mechanistic complexity could be involved in light of the TSA binding experiments, which indicate the potential formation of *bis*-ester-Zn adducts; these are not shown for simplicity and could be relatively unimportant because the substrate ester probably binds with lower affinity than the more basic transition state analog.

Within this mechanistic model the experimentally observed effects of variation of the imine ligand, counterion and sulfonate group on catalytic activity can be accounted for as follows. The irregular correlation between the electronic character, e.g. basicity of the L, X, and $-SO_2R$ groups and the catalytic activity of (imine)ZnX_2 suggests that there is not a common turnover-limiting step (TLS) for all the catalysts. The greater activity of the complexes with less basic imine ligands, e.g. **2g**, **2d** (quinoline) versus **2a** (pyridine), could be the result of outer sphere MeO(H) attack on the electrophilic cationic complex (step 5) being the turnover-limiting step. On the other hand the greater activity of the complexes of more basic imines, e.g. **2b** (imid) > **2a** (pyr), could derive from rate-limiting inner sphere methoxide attack (step 4), enhanced by the greater methoxide nucleophilicity of the (the more electron-rich) **2b**. The apparent steric acceleration observed in some cases, e.g. **2d** > **2g** (i-Pr-quin/quin) and **2h** > **2e** (SO_2Mes/SO_2Tol), is consistent with a step involving decreasing coordination number in or before the TLS, e.g. step 4. The exceptionally low activity of complexes **2c** and **2i** (Ph_2-imid) could be the composite result of lower basicity

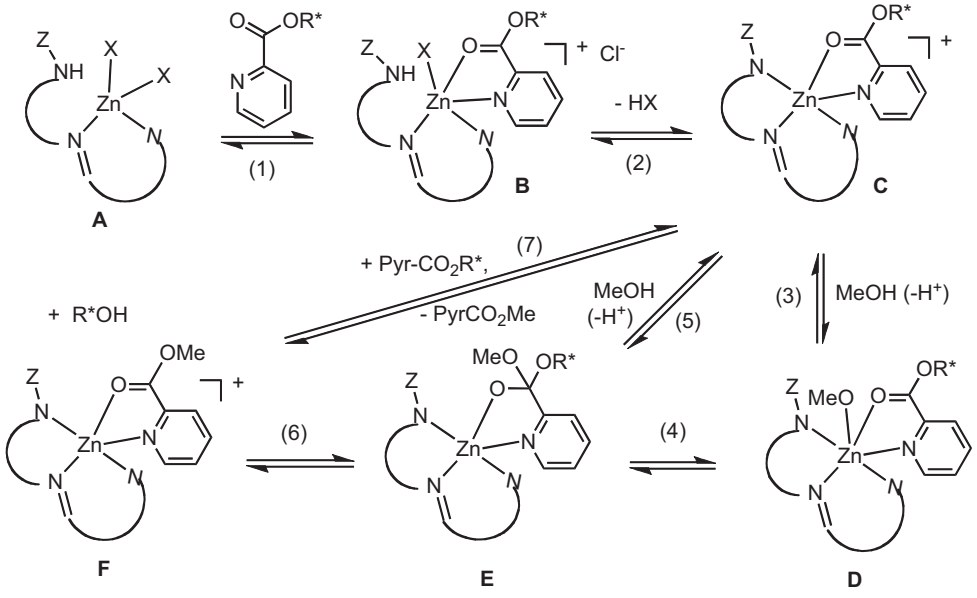

Scheme 4.

of the arylated ligand and increased steric hindrance to external methanol attack (step 3 TLS). These activity-suppressing effects are amplified in **2i** by the weak acidity of the $-SO_2NMe_2$ group, which prevents coordination of the sulfonamide N. The activity dependence on the X anionic ligand variation, i.e. **2d** > **2e** > **2f**, is also unexpected on the basis of basicity/coordinating ability and may again be the result of a changing TLS.

Our preliminary experiments to assess the viability of these complexes as enantioselective catalysts for the kinetic resolution of *rac*-picolinate esters have not been encouraging. The rate constants for methanolysis of the *R*- and *S*-PEP esters with a few of the chiral $LZnX_2$ complexes, e.g. **2h**, were found to be little different, i.e. +10%. Apparently these bi-/tri-dentate ligands fail to provide a sufficiently asymmetric environment to differentiate the diastereomeric transition state s for methanolysis of the chiral picolinate ester. New, more highly ordered ligand–zinc complexes are being sought to remedy this deficiency.

4. Conclusions

We have synthesized novel sulfonamide-based chiral Schiff base–zinc complexes and characterized them by spectroscopic methods. These complexes are active catalysts for the methanolysis of picolinate esters. A substantial difference in catalytic activity is found as a function of the steric and electronic properties of the Schiff base ligand, the coordinating anion, and the potentially coordinating sulfonamide nitrogen. Studies aimed at selecting active catalysts for kinetic resolution by templating a dynamic L-Zn library with transition state analogs are underway in our laboratory.

Acknowledgement

We are grateful for financial support provided by the National Science Foundation (NSF CHE-0911158).

Appendix A. Supplementary data

Supplementary data associated with this article can be found, in the online version, at doi:10.1016/j.molcata.2011.02.014

References

[1] (a) D.W. Christianson, J.D. Cox, Ann. Rev. Biochem. 68 (1999) 33–57;
(b) D.E.A. Raup, B. Cardinal-David, D. Holte, K.A. Scheidt, Nature 18 (2010) 1.
[2] (a) N. Strater, W.N. Lipscomb, T. Klabunde, B. Krebs, Angew. Chem., Int. Ed. Engl. 35 (1996) 2024;
(b) R. Cacciapaglia, A. Casnati, L. Mandolini, D.N. Reinhoudt, R. Salvio, A. Sartori, R. Ungaro, J. Am. Chem. Soc. 128 (2006) 12322.
[3] (a) B.W. Matthews, Acc. Chem. Res. 21 (1988) 333–340;
(b) T. Hofmann, Topics Mol. Struct. Biol. 7 (Metalloproteins, Part 2) (1985) 1–64.
[4] W.N. Lipscomb, N. Strater, Chem. Rev. 96 (1996) 2375.
[5] (a) R.S. Brown, A.A. Neverov, Adv. Phys. Org. Chem. 42 (2008) 271–331;
(b) J. Zhang, X.G. Meng, X.C. Zeng, X.Q. Yu, Coord. Chem. Rev. 253 (2009) 2166–2177;
(c) A.K. Powell, A.C. Deveson, D. Collison, D.R. Harper, F.E. Mabbs, Spec. Publ. – Roy. Soc. Chem. 131 (1993) 82–86;
(d) J. Chin, Acc. Chem. Res. 24 (1991) 145–152.
[6] (a) H. Vahrenkamp, Acc. Chem. Res. 32 (1999) 589;
(b) G. Parkin, Chem. Commun. (2000) 1971;
(c) C. Kimblin, W.E. Allen, G. Parkin, J. Chem. Soc. Chem. Commun. (1995) 1813;
(d) C. Kimblin, G. Parkin, Inorg. Chem. 35 (1996) 6912.
[7] C. Dro, S. Bellemin-Laponnaz, R. Welter, L.H. Gade, Angew. Chem. Int. Ed. 43 (2004) 4479.
[8] (a) T.H. Fife, T.J. Przystas, J. Am. Chem. Soc. 107 (1985) 1041;
(b) L.G. Qiu, X. Jiang, L.N. Gu, G. Hu, J. Mol. Cat. A: Chem. 277 (2007) 15–20;
(c) S.Q. Cheng, Pol. J. Chem. 79 (2005) 933–939.
[9] J.Y. Baek, Y.J. Shin, H.B. Jeon, K.S. Kim, Tetrahedron Lett. 46 (2005) 5143–5147.
[10] T. Sammakia, J.S. Jacobs, Tetrahedron Lett. 40 (1999) 2685–2688.
[11] J.M.J. Williams, R.J. Parker, C. Neri, Enzy. Catal. Org. Synth. 1 (2002) 287–312.
[12] M. Tokunaga, H. Aoyama, J. Kiyosu, Y. Shirogane, T. Iwasawa, Y. Obora, Y. Tsuji, J. Organomet. Chem. 692 (2007) 472.
[13] (a) P.T. Yoon, E.N. Jacobsen, Science 299 (2003) 1691;
(b) C.I. Maxwell, K. Shah, P.V. Samuleev, A.A. Neverov, R.S. Brown, Org. Biomol. Chem. 6 (2008) 2796.
[14] M. Matsumoto, D. Estes, K.M. Nicholas, Eur. J. Inorg. Chem. (2010) 1847.
[15] (a) L. Pauling, Am. Sci. 36 (1948) 51;
(b) W.P. Jencks, Catal. Chem. Enzym. (McGraw Hill) (1969).
[16] J.S. Loran, R.A. Naylor, A.J. Williams, J. Chem. Soc. Perkin Trans. 2 (1976) 1444–1447.
[17] D. Prema, A.V. Wyznicia, B. Scott, J. Hilborn, J. Desper, C. Levy, Dalton Trans. (2007) 4788–4796.
[18] D. Sterk, M.S. Stephan, B. Mohar, Tetrahedron: Asymmetry 13 (2002) 2605–2608.
[19] K. Ng, R. Somanathan, P.J. Walsh, Tetrahedron: Asymmetry 12 (2001) 1719–1722.
[20] (a) J. Y. Liang, N. W. Lipscomb, Carbonic Anhydrase, Proc. Int. Workshop (1991), Meeting Date 1990, 50–64;
(b) M. Remko, J. Mol. Struct. THEOCHEM 944 (1–3) (2010) 34–42.
[21] A. Obreza, S. Gobec, Curr. Med. Chem. 11 (24) (2004) 3263–3278.
[22] R. Kannappan, S. Tanase, I. Mutikainen, U. Turpeinen, J. Reedijk, Polyhedron 25 (2006) 1646–1654.
[23] K. Nakamato, Infrared and Raman Spectra of Inorganic Coordination Compounds, 4th ed., Wiley, New York, 1986, pp. 147, 150, 227, 251 and 253.
[24] Y. Tanaka, J. Org. Chem. 32 (1967) 2405.
[25] A.C.M. Paiva, L. Juliano, P. Boschcov, J. Am. Chem. Soc. 98 (1976) 7645.
[26] (a) D.J. Bowden, S.L. Clegg, P. Brimblecombe, Chemosphere 32 (1996) 405;
(b) A. Behn, M.H. Gordon, A.T. Bell, Organometallics 29 (2010) 1144.
[27] (a) E.G. Kolawole, J.Y. Olayemi, Macromolecules 14 (1981) 1050;
(b) H.S. Kim, J.Y. Bae, J.S. Lee, O.S. Kwon, P. Jelliarko, S.D. Lee, S.H. Lee, J. Catal. 232 (2005) 80–84.
[28] L.M. Berreau, Eur. J. Inorg. Chem. (2006) 273–283.